Письма в ЭЧАЯ. А. 2011. Т. 8, № 9. С. 37–43

STUDY OF CHARGED-PARTICLE CORRELATIONS AND UNDERLYING EVENTS WITH THE ATLAS DETECTOR

C. Bélanger-Champagne
for the ATLAS Collaboration

Institute for Physics and Astronomy, Uppsala University, Uppsala, Sweden

Recent ATLAS measurements of underlying-event properties and charged-particle angular correlations are reviewed. Measurements are done for proton–proton collisions at centre-of-mass energies of 900 GeV and 7 TeV in the pseudorapidity range $|\eta| < 2.5$. The results are compared to various Monte Carlo models and tunes.

PACS: 13.75.Cs; 13.85.-t

INTRODUCTION

Perturbative QCD calculations cannot be done in the so-called «soft» regime, where the transverse-momentum transfer between the initial and final states is small [1]. This regime is thus described in simulation software via empirical models containing many parameters that need to be tuned to data. Improved measurements of quantities dominated by soft QCD effects provide the input necessary to refine the models and retune their parameters. The underlying event (UE) is the term collectively assigned to beam–beam remnants and multiparton interactions (MPI) as well as the initial and final state radiation, which cannot be separated out from the UE on an event-by-event basis. Minimum-bias events [2] are of particular interest for this kind of study as their phenomenology is dominated by soft QCD interactions. Similar studies have also been conducted in the past with dijet and Drell–Yan events [3].

1. DATA SELECTION

The ATLAS detector at the Large Hadron Collider at CERN is described in detail in [4]. The measurements presented use exclusively reconstructed charged-particle tracks which rely on the Inner Detector, the tracking detector closest to the beam pipe. Track reconstruction with the Inner Detector can be done in the pseudorapidity range $|\eta| < 2.5$ down to a transverse momentum p_T of 100 MeV but the results presented here use tracks with $p_T > 500$ MeV.

The minimum-bias event sample used in these analyses was collected using the ATLAS Minimum-Bias Trigger Scintillators (MBTS). This trigger fires upon combined signal-above-background from electrostatic beam pickup timing devices that indicate the presence of proton bunches in the detector and the MBTS, a detector located at ± 3.56 m from the center of the detector along the beampipe. This trigger is $> 99\%$ efficient relative to the off-line

selection of events [2]. The event sample contains proton–proton collision data collected on December 6–15, 2009 for 900 GeV collisions and on March 30 – April 27, 2010 for 7 TeV collisions. Events that passed the trigger where also required to contain one well-reconstructed primary vertex (PV) but are vetoed if they contain other PV candidates with at least 3 associated tracks.

The following selection is then applied to individual tracks: each track must have $p_T > 500$ MeV, at least 1 Pixel detector hit and 6 silicon microstrip hits including 1 hit in the first Pixel layer if the module was active, transverse and weighted longitudinal parameters (respectively $|d_0|$ and $|z_0| \sin\theta$) < 1.5 mm and, for tracks with $p_T > 10$ GeV, the track fit χ^2 probability must be greater than 0.01, to protect against mismeasured tracks. For the underlying event analysis, a further requirement that at least one track has $p_T > 1$ GeV is applied.

2. UNDERLYING EVENT MEASUREMENTS

For a charged particle with azimuthal angle ϕ in the transverse plane of the detector, the magnitude of the azimuthal angular difference to the leading track is given by $|\Delta\phi| = |\phi - \phi_{\rm lead}|$. To create regions of $\eta - \phi$ space that are sensitive to different aspects of the UE, three equal regions are defined in $|\Delta\phi|$: toward ($|\Delta\phi| < 60°$), transverse ($60 < |\Delta\phi| < 120°$) and away ($|\Delta\phi| > 120°$). Various quantities are then measured separately for each region. The transverse region phenomenology is dominated by the UE.

Corrections are applied to make measurements comparable to particle–level Monte Carlo (MC). First, an event-level correction weight is applied. It is given by

$$w_{\rm ev} = \frac{1}{\epsilon_{\rm trig}(N_{\rm sel}^{\rm BS})} \frac{1}{\epsilon_{\rm vertex}(N_{\rm sel}^{\rm BS}, \langle\eta\rangle)} \frac{1}{\epsilon_{\rm lead\ track}(\epsilon_{\rm track})}, \quad (1)$$

where $N_{\rm sel}^{\rm BS}$ is the number of selected tracks relative to the beamspot with a transverse impact parameter < 1.8 mm, $\epsilon_{\rm trig}(N_{\rm sel}^{\rm BS})$ is the trigger efficiency, $\epsilon_{\rm vertex}(N_{\rm sel}^{\rm BS}, \langle\eta\rangle)$ is the vertex finding efficiency and $\epsilon_{\rm lead\ track}(\epsilon_{\rm track})$ is the efficiency for finding a leading track. A track-level correction is then applied, given by

$$w_{\rm track} = \frac{1}{\epsilon_{\rm track}(p_T, \eta)} (1 - f_{\rm sec}(p_T))(1 - f_{\rm okr}(p_T, \eta))(1 - f_{\rm fake}), \quad (2)$$

where $\epsilon_{\rm track}(p_T, \eta)$ is the tracking efficiency as described in [5]; $f_{\rm sec}(p_T)$ is the fraction of secondaries; $f_{\rm okr}(p_T, \eta)$ is the fraction of selected tracks for which the corresponding primaries are outside of the kinematic range, and $f_{\rm fake}$ is the fraction of fake tracks. Finally, bin-by-bin unfolding is applied to account for bin-to-bin migrations and event reorientation due to missing or misidentified leading tracks. The unfolding factor is found to be within 10% of unity in the lowest leading track p_T bins and smaller for higher leading track p_T bins. The unfolding procedure has an associated systematic uncertainty of approximately 2% in the plateau region due to the choice of MC model and limited MC statistics. Significant systematic uncertainties arise also via the efficiency correction procedures at event and track level. The systematic uncertainties are summarized in Table 1.

The density of charged particles and their mean p_T as a function of leading track p_T in the transverse region at 900 GeV and 7 TeV are shown in Fig. 1 and compared to predictions

Table 1. **Systematic uncertainty table for the 7 TeV (900 GeV) results**

Parameters	Lowest p_T bins	Highest p_T bins
From unfolding		
Difference between generators, %	4	2
Statistical uncertainty on MC sample,%	< 0.1	4 (5)
From efficiency corrections		
Tracking efficiency, %	3	4
Leading track requirement, %	1	< 0.1
Trigger and vertexing, %	< 0.1	< 0.1
Total systematic uncertainty, %	4.5	6 (6.5)

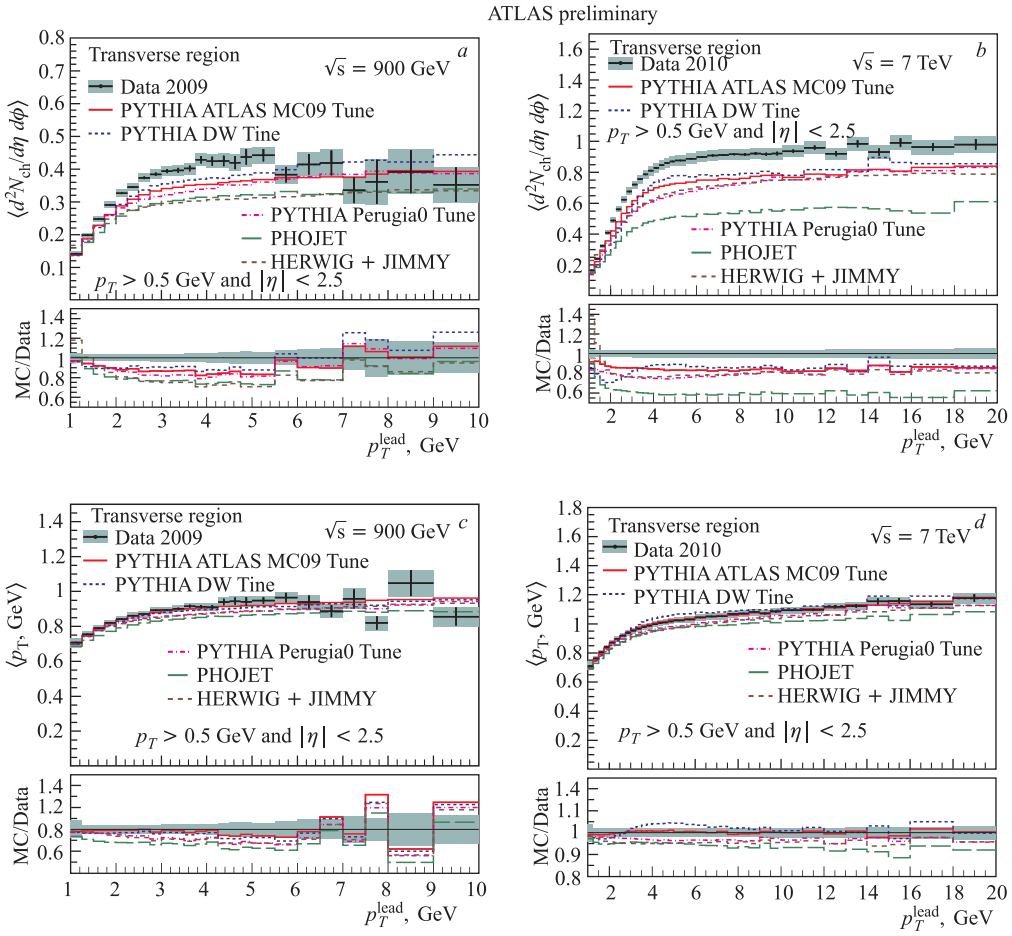

Fig. 1. Density of charged particles $\langle d^2N_{\rm ch}/d\eta\, d\phi\rangle$ as a function of leading track p_T in the transverse region at 900 GeV (*a*), at 7 TeV (*b*). Mean p_T of charged particles as a function of leading track p_T in the transverse region at 900 GeV (*c*) and at 7 TeV (*d*). The error bars show statistical uncertainties while the shaded rectangles show the quadratic sum of statistical and systematic uncertainties

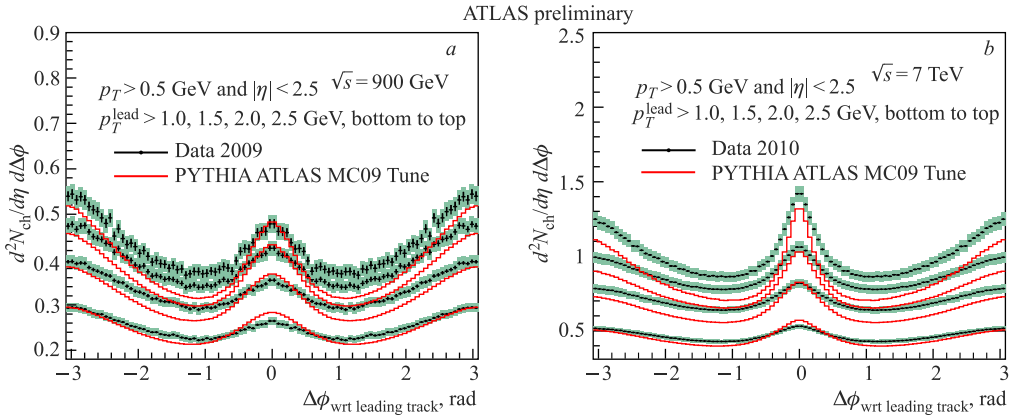

Fig. 2. $\Delta\phi$ distribution of track densities $d^2N_{\text{ch}}/d\eta\, d\Delta\phi$ relative to the leading track, with varying leading track p_T minimum at 900 GeV (*a*) and 7 TeV (*b*). Distributions are symmetrized around $\phi = 0$, the bars show statistical uncertainties while the shaded rectangles show quadratically summed statistical and systematic uncertainties

from multiple PYTHIA [6] tunes as well as to PHOJET [7] and HERWIG + JIMMY [8]. All PYTHIA tunes predict 10–15% lower density of charged particles than observed in the plateau region at both energies, and the other generators present a worse match to data. The toward and away regions (not shown) are better described, and PYTHIA Tune DW [9] is the closest match to the data. Similarly, for $\langle p_T \rangle$, the MC predictions are somewhat lower than the data in the plateau region at both energies.

The angular distribution of charged particle relative to the leading track is shown in Fig. 2 for multiple leading track p_T requirements. As expected, the increased p_T requirement on the leading track highlights the development of jet-like structure at $\Delta\phi = 0$ and π. Large differences in shapes are observed when compared to MC. More measurements and a detailed description of the analysis can be found in [10].

3. ANGULAR CORRELATION MEASUREMENTS

A complementary approach to the study of angular correlations shown in Fig. 2 is presented in this section. It focuses on isolating the peaking structure of the distribution while minimizing the influence of systematic uncertainties [11, 12].

The crest shape observable is constructed from a basic $\Delta\phi$ track density distribution as in Fig. 2 but without symmetrization and with the leading track $p_T > 500$ MeV. In this distribution, each bin contains N^T tracks. A second-order polynomial function is fitted to the area around the minimum of $\Delta\phi$, and the value of the fitted minimum (N^T_{min}) is subtracted from each bin. The area of the resulting distribution is then normalized to unity. The crest shape resulting from these manipulations can be expressed as $(N^T - N^T_{\text{min}})/\sum(N^T - N^T_{\text{min}})/(\pi/50)$ and is shown in Fig. 3, *a* and *c*.

To create the «same minus opposite» distribution, the basic $\Delta\phi$ distribution is constructed separately for tracks that, event-by-event, have pseudorapidity of the same sign as the leading track in that event, or the opposite sign as the leading track, resulting in

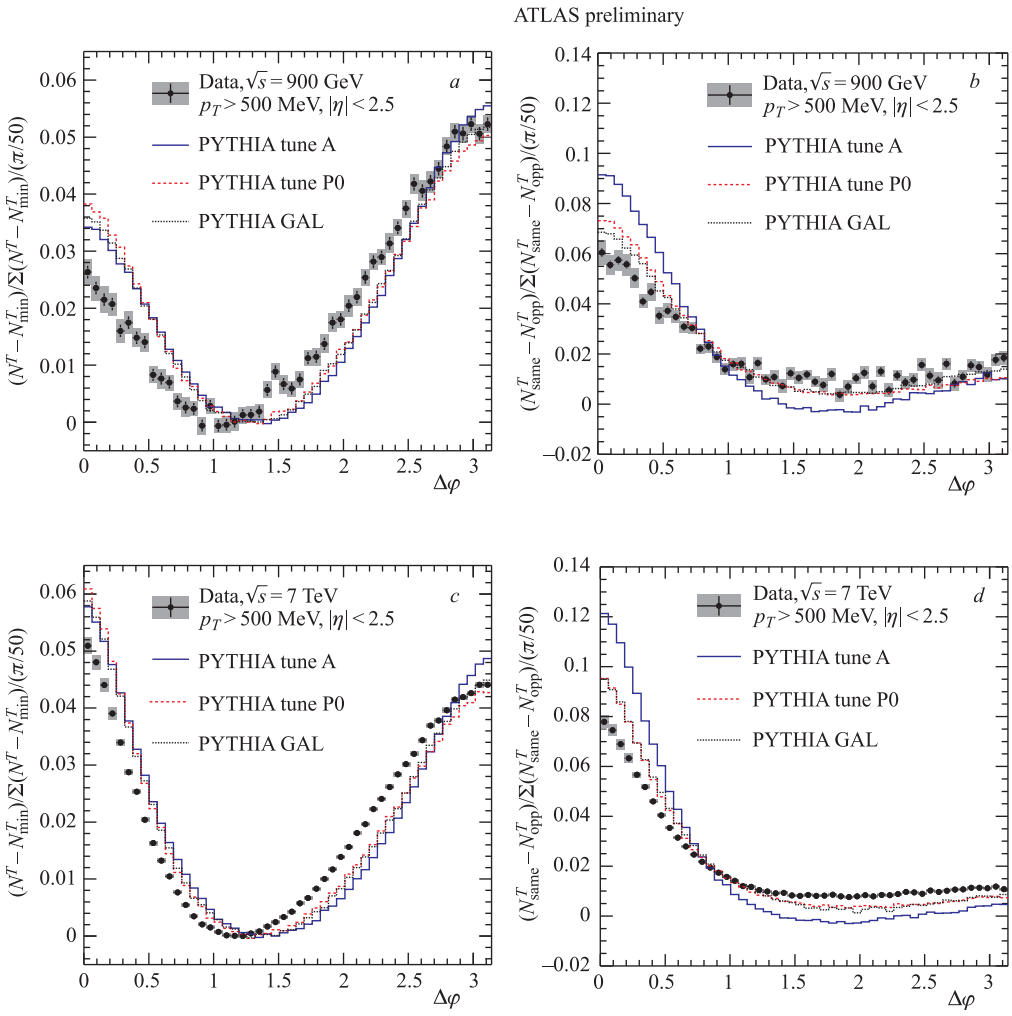

Fig. 3. Measured distributions and comparisons to MC distributions at 900 GeV for the crest shape (*a*) and the «same minus opposite» observable (*b*) and at 7 TeV for the crest shape (*c*) and the «same minus opposite» observable (*d*). The error bars display the statistical uncertainty while the filled rectangles are the sum, in quadrature, of statistical and systematic uncertainties

N^T_{same} and N^T_{opp} histograms, respectively. The «opposite» distribution is subtracted from the «same» distribution and the result is normalized to unity. This can be expressed as $(N^T_{\text{same}} - N^T_{\text{opp}})/\sum(N^T_{\text{same}} - N^T_{\text{opp}})/(\pi/50)$ and is shown in Fig. 3, *b* and *d*. The observables constructed in this way are remarkably robust against experimental and detector effects. Without any corrections, the agreement in simulated events between distributions obtained from generated particles and reconstructed tracks is better than 5% close to 0, where the discrepancy is largest.

As with the underlying event, a track-level correction given by Eq. 2 is applied. A second shape correction to offset the effect of the loss of leading tracks is applied. The corrected

distribution is obtained by extrapolating back, bin-by-bin in the distribution, to 100% leading track efficiency using data distributions where observed leading tracks have been removed. This second correction improves the agreement between generated and reconstructed MC distributions in the whole $\Delta\phi$ range except for the first few bins, where closure tests show that the correction biases the extrapolation up by 2%. This bias is taken as a systematic uncertainty in the first four bins.

Table 2. **Systematic uncertainties table for angular correlations measurements at 7 TeV (900 GeV)**

Source of systematic uncertainty, %	Relative uncertainty in the first bins
Event selection	1 (3)
Leading track correction bias	2 (first 4 bins)
Kinematic cuts — resolution	1 (2)
Misidentified leading tracks	0.1 (0.2)
Tracking efficiency, leading tracks	0.1 (0.2)
Tracking efficiency, nonleading tracks	0.2
Tracking efficiency, ϕ dependence	0.1 (0.2)
Contamination by fakes	0.1 (0.3)

Systematic uncertainties are summarized in Table 2. Most are found to be largest close to zero. Systematic uncertainties associated to the efficiency of event selection, kinematic cuts and fake contamination were measured by varying the appropriate selection cuts. The effect of misidentifying the leading track was estimated in MC to be small and as an associated systematic uncertainty of 0.1–0.2%. Systematic uncertainties associated with the tracking efficiency correction procedures were measured by carrying the procedure again while varying the efficiency within its systematic range. The tracking efficiency dependence on the detector location in ϕ was measured by quantifying the variation of the number of tracks in ϕ in data, as physical processes are ϕ-independent. Finally, the tracking efficiency difference between the two halves of the detector was found to have a negligible effect on the measurement of the «same minus opposite» distribution.

Comparisons of the measured observables in data with three PYTHIA tunes are shown in Fig. 3 for both observables at both collision energies. The PYTHIA tunes present a wide range of predictions, yet none matches the data distributions. If the measurement is restricted to the range $|\eta| < 1$ (not shown), where tuning data CDF [3] is available, the tunes lie closer together and behave a lot more like data, as expected. More PYTHIA tunes than those presented were tested, and among them tune PHARD was found to lay closest data. It is still not, however, a quantitatively good match. Complete results can be found in [12].

4. SUMMARY

Two series of ATLAS results on soft QCD physics were presented. All existing underlying-event models predicted lower activity level and $\langle p_T \rangle$ than were observed for both collision energies. These and other UE observables help constrain the energy evolution of MPI models. The observed discrepancies indicate that extrapolation parameters in current models fail to accurately predict behaviour at LHC energies. Angular correlations and the emergence of jet structure are particularly poorly described. The importance of these results becomes apparent

as they constitute input data to new models and tunes of the UE and soft QCD in MC generators which can then be fed back into the analysis chain and benefit all physics measurements at the LHC.

REFERENCES

1. *Ellis R. K., Stirling W. J., Webber B. R.* QCD and Collider Physics // Camb. Monogr. Part. Phys. Nucl. Phys. Cosmol. 1996. V. 8. P. 435.
2. *ATLAS Collab.* // Phys. Let. B. 2010. V. 688. P. 21–32.
3. *CDF Collab.* // Phys. Rev. D. 2010. V. 82.
4. *ATLAS Collab.* // JINST. 2008. V. 3. P. S08003.
5. *ATLAS Collab.* ATLAS-CONF-2010-046. 2010.
6. *Sjöstrand T. et al.* // JHEP. 2006. V. 05. P. 026.
7. *Engel R.* // Z. Phys. C. 1989. V. 66 P. 203–214.
8. *Corcella C. et al.* arXiv:hep-ph/0210213.
9. *Field R.* Min-Bias and the Underlying Event at the Tevatron and the LHC. Talk presented at the FERMILAB MC Tuning Workshop, FERMILAB. 2002.
10. *ATLAS Collab.* ATLAS-CONF-2010-081. 2010.
11. *D0 Collab.* D0 Note 6054-CONF. 2010.
12. *ATLAS Collab.* ATLAS-CONF-2010-082. 2010.